Application of optimized photovoltaic grid-connected control system based on modular multilevel converters

Jun Xie[1*]

*Correspondence:
XIEJUN20240312@163.com

[1] School of Intelligent Manufacturing, Anhui Vocational and Technical College, Hefei 230011, China

Abstract

Photovoltaic power generation is a promising method for generating electricity with a wide range of applications and development potential. It primarily utilizes solar energy and offers sustainable development, green environmental benefits, and abundant solar energy resources. However, there are many external factors that can affect the output characteristics of Photovoltaic cells and the effectiveness of the grid-connected control system. This study describes the introduction of Modular Multilevel Converter (MMC) technology into photovoltaic power generation systems to improve power generation efficiency. It proposes optimizing and improving the technology by adjusting the temperature and magnitude of lighting and combining traditional algorithms to propose a composite control algorithm. The photovoltaic power generation system employs the modular multi-level converter technology to enhance power generation efficiency alongside optimization and improvement. The temperature and size of light are regulated alongside the traditional algorithm to introduce the composite control algorithm. The improved composite algorithm surpasses the traditional one after experimental comparison of the results. The testing of a model photovoltaic power grid-connected system shows that the combination of modular multi-level converter technology and a photovoltaic grid-connected system, incorporating composite proportional integral control and quasi-proportional resonant control algorithms, yields improved results and feasibility. With rationality and effective control. The simulation results show that at 0.5 s, the light intensity suddenly increases from 750 to 1000 W/m^2, and the direct-current voltage suddenly increases for a short time, but then decreases rapidly and finally returns to a stable level close to the rated voltage. From this, it can be seen that when the light intensity continues to change, the voltage value on the direct-current bus side of this MMC grid-tied photovoltaic system can still be maintained close to the rated value, ensuring the operational stability of the entire system. Sensibly and effectively controlled. The implementation of MMC technology in photovoltaic power generation systems enhances power generation efficiency, whilst simultaneously supporting the advancement of photovoltaic power generation and contributing towards environmental protection in the long term.

Keywords: Modular multi-level converter technology converter, Grid-connected control system, Fixed Voltage algorithm, Photovoltaic cells

Introduction

Photovoltaic (PV) power generation technology is green, environmentally friendly and sustainable, and in the context of the energy crisis, PV power generation research is of great significance in the international arena (Xu et al. 2021). Energy issues affect the strength of a country's economy and are closely related to the standard of living of its people (Pillai 2021). The development and use of new energy sources such as renewable wind, solar and tidal power will be a topic of far-reaching research in the future, and the development and utilization of new energy sources will have an impact on the production capacity of society (Xiu and Zhao 2021). With the rapid development of industry, the demand for energy is increasing, and the storage capacity of non-renewable resources is gradually decreasing, so green renewable resources are the focus of research by scholars at home and abroad (Wang et al. 2021; Li et al. 2021; Islam et al. 2021). Many environmental factors that exist in the outside world can have an impact on the PV power generation method, which can affect the output characteristics of PV power generation and the effectiveness of the grid-connected control system, resulting in poor effectiveness (Liu et al. 2021). In order to improve the transmission capacity and efficiency in PV power systems, modular multilevel converter (MMC) grid-connected inverters have significant advantages in terms of total installed capacity, harmonic content and system voltage (Ma et al. 2021). The MMC converter performs better in many aspects compared to the conventional type of inverter. To better adapt to the complexity and uncertainty of PV power generation systems, a control algorithm based on composite proportional integral control and quasi-proportional resonance control is proposed. This algorithm is tailored to the specific characteristics of PV power generation systems, allowing for improved adaptation to their complexity and uncertainty. To verify its effectiveness, the performance of the PV grid-connected system model is tested, its stability and feasibility are analyzed, and it is compared with the traditional algorithm.

This study is separated into five parts, the first part provides an overview of the research background and summarizes the research in related fields. The second part describes the specific methodology of adding MMC for optimizing the PV grid-connected control system. The third part verifies the effectiveness of the optimized PV grid-connected cell and experimentally verifies the feasibility of the improved composite algorithm obtained. The five part summarizes and outlooks the whole research. The last part is a brief discussion of the results obtained in the paper.

Related works

In response to some problems of MMC converters, many scholars have conducted various types of studies and explorations on them. Lei et al. conducted an in-depth study on the circuit dynamics and control strategy of a full-bridge five-branch MMC, and identified its potential application in integrated power quality management of an in-phase railway power system under a detailed consideration of the non-ideal operating conditions (Lei et al. 2022). Conventional multi-terminal hybrid microgrids based on multilevel converters required a large number of power switches and have limited operational capability under unbalanced power distribution in low- and medium-voltage (LV) microgrids. A novel five-terminal LV and medium-voltage (MMC) hybrid AC/DC

microgrid based on MMCs was been proposed by Xiao et al. The proposed topology significantly reduced the number of power switches compared to conventional MMC-based hybrid microgrids (Xiao et al. 2022a). Inwumoh et al. proposed a new control structure to ensure proper dynamic response, balance the internal energies of the arms and legs, minimize dc oscillations, and provide DC-FRT capability along with static synchronous compensation. The results under normal and inter-pole DC faults were analyzed to validate the proposed control scheme (Inwumoh et al. 2022). MMC become prominent in high and medium power applications. The phase configured pulse width modulation technique is a carrier based method that produces high quality output. However, there was an inherent problem of uneven power distribution. Gobburi et al. proposed a capacitor voltage balancing method for MMC which eliminates the need for voltage and current sensors (Gobburi et al. 2022).

Many scholars have conducted research on improving the system optimization of PV power generation and resolving the influencing factors present therein. Guo et al. proposed the application of a copula function to describe the correlation between wind and PV power generation to solve the problem of a high proportion of renewable energy sources being connected to the grid endangering the safe operation of the power system (Guo et al. 2022). And the uncertainty of the operation of the power system with high percentage of renewable energy was reduced. To improve the robustness of the model, it was proposed to apply the conditional value-at-risk theory to construct the objective function of the model, which effectively controls the tail risk of the operating cost of the power system. The experimental results showed that the proposed model was highly practical and economical (Ju et al. 2022). To solve the problem of unstable voltage and intermittent power generation in PV power systems often due to shade, dust, rain, etc., which leads to unstable power quality and failure of equipment connected to the system, Chen et al. came out with a hybrid energy storage module and precise control strategy for PV power systems. Brushless DC motors were connected to the system to study the extent of improvement in power quality and runtime. The experimental results showed that the system had a sustainable power supply and the PV power generation system with the proposed hybrid energy storage module and control strategy effectively reduced voltage instability and power generation interruptions and improves power quality (Chen et al. 2022). Existing research on the reliability of phased mission systems mainly focuses on internal failures. However, some practical phased mission systems, such as PV-based power generation systems, may also be subject to external influences. Xiao et al. modeled the reliability of PV-based power generation systems considering both internal failures and external influences affecting the failure rate of PV modules. In modelling the system reliability, two different scenarios were considered to further optimize the configuration of the PV array and the protection of each PV module to improve the reliability of the system (Xiao et al. 2022b). In order to address the safety of lightning protection systems in PV power generation for severe weather conditions such as thunderstorms, Rugthaicharoencheep and Maigan developed a simple model of PV power generation which includes the arrangement of conventional PV panels. The effects of lightning can also be modeled by the pattern of lightning current. The dimensions of the panel mounting structure and the lightning conduction points induce induced voltages at the joints of the PV panels. According to the results of the inrush current analysis,

the intensity of the lightning current was increasing rapidly (Rugthaicharoencheep and Maigan 2020). When the PV system was connected to the grid, the nonlinear load of the grid affected the power quality and consumed reactive power. To solve this problem, Gong et al. proposed a grid-connected PV power system with an active power filter function to improve the power quality. The PV power generation can be operated at the maximum power point through the maximum power point tracking (MPPT) method and perform the functions of harmonic and reactive power compensation at the load side. The validation results showed that the system injected maximum power into the grid while the load varies and compensates the harmonics generated by the nonlinear loads in the grid, so that the total harmonic distortion (THD) of the grid meets the operation standard, i.e., the system had good dynamic and steady state performance (Gong et al. 2021). Meenalochini and colleagues advanced single source cascaded H-bridge multi-level inverter (MLI) technology by introducing self-balancing series/parallel switched capacitors (SCs). This development generated additional output levels in the MLI. The utilization of asymmetric characteristics in H-bridges allows for the provision of levels with varying voltage intervals. Consequently, cascading MLIs only necessitates one DC power supply and fewer components for the generation of multiple levels. In comparison to traditional asymmetric cascaded MLI, the proposed MLI reduces the need for multiple power supplies, whilst ensuring automatic balancing of capacitor voltage. The incorporation of SC technology facilitates an increase in boost capacity and output levels (Ye et al. 2020). Norman and colleagues have put forward three distinct topologies for grid connected PV applications: a three-phase cascaded H-bridge MLI topology, a three-phase cascaded voltage source inverter topology featuring inductors, and a three-phase cascaded voltage source inverter topology utilizing coupling transformers. The research compared three topology structures based on the number of switches, voltage and current stress exerted on the switches, THD of the generated voltage and grid current, and efficiency using experiments and simulations. This article validates the efficiency and dependability of the proposed topology structure via simulation, experimental results, and comparison (Noman et al. 2019).

In summary, many scholars have investigated the circuit dynamics and control strategies of MMC converters and PV power generation fields. However, existing studies have limitations in ensuring the stability and efficiency of MMC converters under non-ideal operating conditions. This study introduces the optimized PV grid-connected control of MMC for non-ideal operating conditions to ensure the stability and efficiency of the MMC converter. The introduction of the MCC converter into the PV grid-connected control system to optimize the system is one of the more innovative research directions.

Exploration of photovoltaic cell simulation technology and control strategy for improved structure of MMC converter

By analyzing the working principle of PV cell, the mathematical model of PV cell is established, and a composite MPPT control strategy is proposed, according to the mathematical model of PV cell, which can be converted into the form of equivalent circuit for analysis, and the PV cell is obtained when it is at different working points. Equivalent circuits are obtained at different operating points of the PV cell.

Modeling of PV cells and their MPPT control strategies

A mathematical model for solar PV cells is proposed, and an engineering practical model is built using MATLAB/Simulink simulation software. Figure 1 shows the internal structure diagram of the MATLAB/Simulink simulation circuit for the PV cell.

Figure 1 shows that the PV cells are PN junction type PV cells. Electrons and holes near the PN junction region diffuse into each other, forming a built-in electric field in the PN junction region pointing from the N region to the P region. The sun's rays are absorbed by the PV cell, and photons with sufficient energy excite electrons from covalent bonds in the P- and N-type silicon, creating electron–hole pairs. The commonly used semiconductor materials are monocrystalline silicon, polycrystalline silicon, and amorphous silicon. Thus, solar PV cells consist mainly of monocrystalline silicon and polycrystalline silicon PV cells, among others (Subudhi and Punetha 2023). Semiconductors are the primary component of solar PV cells. At present, the most effective solar PV cells are the monocrystalline silicon PV cells that are widely used. The working principle of the solar PV cells is illustrated in Fig. 2.

As illustrated in Fig. 2, PV solar cells operate through a PN junction, a semiconductor device that generates a photogenerated electromotive force in response to sunlight. The force moves in the opposite direction of the electric field, creating a positive charge in the P region and a negative charge in the N region. Voltage reactions will take place between the N and P regions, producing electrical energy and achieving the conversion of solar energy into electrical energy. PV power generation medium for PV cells, PV cell internal structure is the basic content of PV power generation, the equivalent circuit diagram of the battery is shown in Fig. 3.

As shown in Fig. 3, the main components of the circuit are: a PV current source, three resistors, and a parallel diode. In the Fig. 3, I_L represents the load current of the PV cell, I_{ph} represents the input current of the PV cell, I_d represents the current on the diode branch, and U represents the total voltage in the circuit. Calculation formulas are used to compare differences between experimental conditions or data.
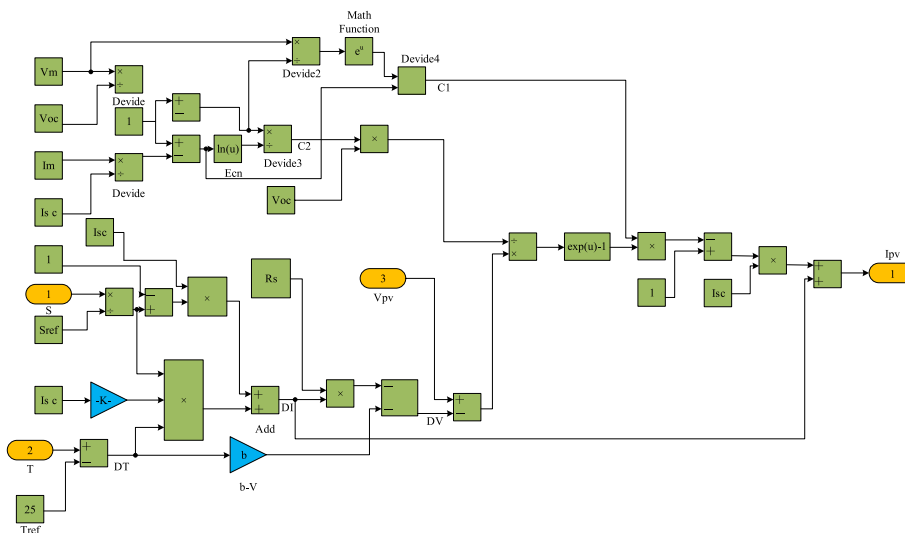
Fig. 1 MATLAB/Simulink simulation circuit internal structure of photovoltaic cell
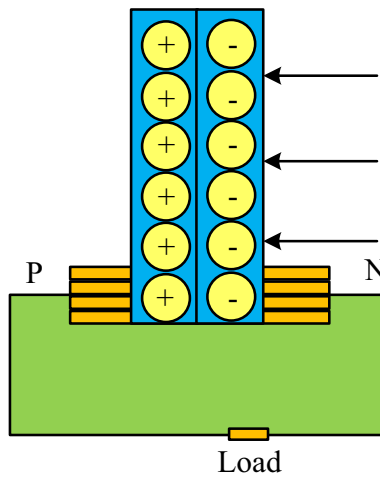
Fig. 2 Photovoltaic effect diagram
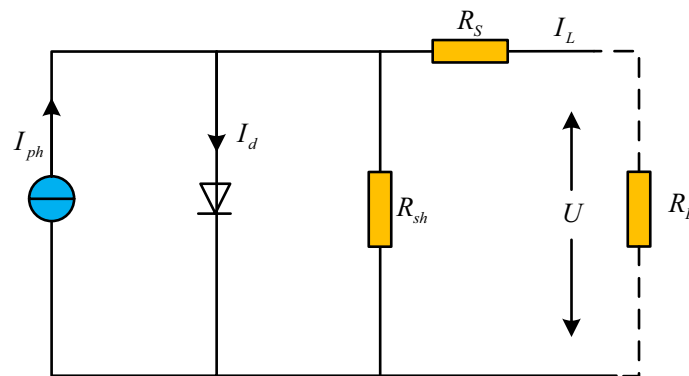
Fig. 3 Single diode equivalent circuit of photovoltaic cells

This provides a basis for subsequent experiments and allows for the assessment of the influence of various factors on the results. The current of diode I_d is calculated as shown in Eq. (1).

$$I_d = I_0 \left[\exp(\frac{qU}{AkT}) - 1 \right] \tag{1}$$

The load current I_L is calculated as shown in Eq. (2).

$$I_L = I_{ph} - I_0 \left(e^{\frac{q(U_L + I_L R_s)}{AkT}} - 1 \right) - \frac{U_L + I_L R_s}{R_{sh}} \tag{2}$$

As shown in Eq. (2), the resistances of R_s and R_{sh} are determined by the internal material of the cell. And the resistance value of R_s is very small, and the resistance value of R_{sh} is very large, so the resistance of R_s can be ignored, and the shown Eq. (2) can be expressed as Eq. (3).

$$\begin{cases} I_L = I_{ph} - I_0 \left(e^{\frac{qU_L}{e^{AkT}}} - 1 \right) \\ U_L = \frac{AkT}{q} \ln \left(\frac{I_{ph} - I_L}{I_0} + 1 \right) \end{cases} \tag{3}$$

As shown in Eq. (3), when the short-circuit experiment, $R_L = 0$, at this time, the output current of the battery I_L is equal to the short-circuit current I_{sc}. In the open-circuit experiment, R_L value of positive infinity, the voltage at both ends of the battery is expressed as U_{oc}, in the form of a formula as shown in Eq. (4).

$$U_{oc} = \frac{AkT}{q} \ln \left(\frac{I_{ph}}{I_0} + 1 \right) \approx \frac{AkT}{q} \ln \left(\frac{I_{ph}}{I_0} \right) \tag{4}$$

As shown in Eq. (4), the open-circuit voltage is U_{oc} influenced by factors that are directly proportional to the intensity of sunlight and inversely proportional to the outside temperature, and in practice, the expression of I_L I_L is shown in Eq. (5).

$$I_L = I_{sc} \left[1 - C_1 \left(e^{\frac{U_L}{C_2 U_{oc}} - 1} \right) \right] \tag{5}$$

When the open circuit experiment is carried out, the output current of the solar PV cell is 0, the voltage at both ends of the solar PV cell U_{oc}, and when the solar PV cell is operated at maximum power, the output current I_m the voltage at both ends of the solar PV cell is U_m. The expressions of C_1 and C_2 can be obtained as shown in Eq. (6).

$$\begin{cases} C_1 = \left(1 - \frac{I_m}{I_{sc}} \right) e^{-\frac{U_m}{C_2 U_{oc}}} \\ C_2 = \left(\frac{U_m}{U_{oc}} - 1 \right) \left[\ln \left(1 - \frac{I_m}{I_{sc}} \right) \right]^{-1} \end{cases} \tag{6}$$

Since solar light and temperature variations have an effect on current and voltage, the presence of temperature difference ΔT and light temperature ΔS is shown in Eq. (7).

$$\begin{cases} \triangle T = T - T_{ref} \\ \triangle S = \frac{S}{S_{ref}} - 1 \end{cases} \tag{7}$$

As shown in Eq. (7), T_{ref} represents the high standard temperature of the external environment and S_{ref} represents the standard solar radiation intensity. Therefore the characteristic equation of solar PV cell considering the solar radiation intensity and ambient temperature variation is shown in Eq. (8).

$$\begin{cases} I_{sc}^* = I_{sc} \frac{S}{S_{ref}} (1 + \alpha \triangle T) \\ U_{oc}^* = U_{oc} (1 - \delta \triangle T) \ln(1 + \beta \triangle S) \\ I_m^* = I_m \frac{S}{S_{ref}} (1 + \alpha \triangle T) \\ U_m^* = U_m (1 + \delta \triangle T) n (1 + \beta \triangle S) \end{cases} \tag{8}$$

The equivalent circuit of the MMC can be directly connected to the AC side through a transformer, and each sub-module of the MMC operates on the same principle and can be controlled independently, and the three-phase bridge arms are completely symmetrical and independent of each other. The voltages of the upper and lower bridge arms are calculated as shown in Eq. (9).

$$
\begin{cases}
i_{pj} = i_{zj} + \dfrac{i_{vj}}{2} (j = a, b, c) \\
i_{nj} = i_{zj} + \dfrac{i_{vj}}{2} (j = a, b, c)
\end{cases}
\tag{9}
$$

As shown in Eq. (9), i_{zj} is the internal current of the upper and lower bridge arm converters. The two equations are subtracted as shown in Eq. (10).

$$
i_{zj} = \frac{i_{pj} + i_{nj}}{2}
\tag{10}
$$

As shown in Eq. (10), i_{zj} is the internal current of the upper and lower bridge arm converters. i_{pj} is the internal current of the upper bridge arm, i_{nj} is the internal current of the lower bridge arm. Since the simplified circuit collaborates the loop formed by the upper and lower bridge arms of the MMC and the AC output with the KVL equation as shown in Eq. (11).

$$
\begin{cases}
u_{vj} = \dfrac{U_{dc}}{2} - u_{pj} - L\dfrac{di_{pj}}{dt} - Ri_{pj} \\
i_{nj} = u_{nj} + L\dfrac{di_{nj}}{dt} + Ri_{pj} - \dfrac{U_{dc}}{2}
\end{cases}
\tag{11}
$$

As shown in Eq. (11), U_{dc} represents the DC measured voltage of the MMC, and u_{nj} represents the output voltage of the j phase. The mathematical model equation of the MMC is shown in Eq. (12).

$$
\begin{cases}
u_{vj} = \dfrac{u_{nj} - u_{pj}}{2} - \dfrac{R}{2}i_{vj} - \dfrac{L}{2}\dfrac{d_{vj}}{dt} \\
L\dfrac{di_{nj}}{dt} + Ri_{pj} = \dfrac{U_{dc}}{2} - \dfrac{u_{pj} + u_{nj}}{2}
\end{cases}
\tag{12}
$$

In Eq. (12), u_{vj} denotes the output voltage of phase j, u_{pj} denotes the input voltage of phase j. i_{vj} denotes the internal current of the upper bridge arm converter and i_{nj} denotes the internal current of the lower bridge arm converter. The modified MMC output voltage equation is shown in Eq. (13).

$$
u_{vj} = \frac{\sum\limits_{k=1}^{N} (S_{njk}u_{cnjk} - S_{pjk}u_{cpjk})}{2} - \left(\frac{L}{2}\frac{di_{vj}}{dt} + \frac{R}{2}i_{vj} \right)
\tag{13}
$$

The AC measurement input voltage magnitude needs to be satisfied as shown in Eq. (14).

$$u_{vj} \in \left[-\frac{U_{dc}}{2}, +\frac{U_{dc}}{2} \right] \tag{14}$$

The voltage regulation system is defined as Eq. (15).

$$m = \frac{2U_{mj}}{U_{dc}} \tag{15}$$

Control strategies and improved composite control algorithms for photovoltaic power generation systems

The PV cell is equivalent to a non-linear DC power supply. When the output voltage does not reach the previous peak value, the output current remains basically unchanged, equivalent to a constant current source, but when the output voltage exceeds the peak value, the output current will decrease rapidly with the increase in voltage until it decreases to zero. During this process it can be approximated to a constant voltage source due to the rapid reduction of current to zero and the small range of voltage variation. Before the peak voltage is reached, the output power will increase slowly. When the peak voltage is exceeded, the output power will decrease rapidly until it reaches zero (Naz et al. 2023). Therefore, it can be concluded that there is only one point of maximum output power when the external ambient temperature and solar radiation intensity are certain. PV grid-connected power generation in the important role of components, solar PV cell conversion rate needs to be improved, for the problem, the need to first of all PV array conversion efficiency, and also into the control structure of the inverter. In order to ensure that the cells always operate near the maximum power point, the operating point of the PV array needs to be constantly adjusted in real time. This MPPT behaviour is implemented in the study using the fixed voltage method and the perturbation observation method. The algorithmic control flowchart for the maximum voltage method is shown in Fig. 4.

As shown in Fig. 4, firstly, the system obtains the voltage at the output port of the solar PV cell as U_{pv}, compares U_{pv} with the voltage reference value of the solar PV cell U_{pv}^*, and when the output voltage value is equal to the reference voltage value, then the output voltage is kept unchanged and outputs it. If the output voltage is different from the reference voltage, it is necessary to use the control system to regulate the output voltage so that the two are equal, and then it will be output.

This study employs a fixed voltage tracking algorithm to select U_{pv} and U_{pv}^* parameters for regulating the output voltage of the MMC multistage converter. This approach enables precise control of the MMC multistage converter, thereby improving the performance and stability of the PV grid-connected control system. However, the application of PV cells can be influenced by temperature when utilizing the fixed voltage tracking method in practical settings. Moreover, the instability of the PV battery use in such environments causes U_{oc} to fluctuate. This leads to the conclusion that the fixed voltage method is disadvantageous, as it lacks the accuracy required to adjust to changing environments. Additionally, this technique tends to incur a higher power loss compared to other methods. Thus, in modern industry, it is almost impossible to solely rely on the fixed voltage method. The disturbance observation method is widely used
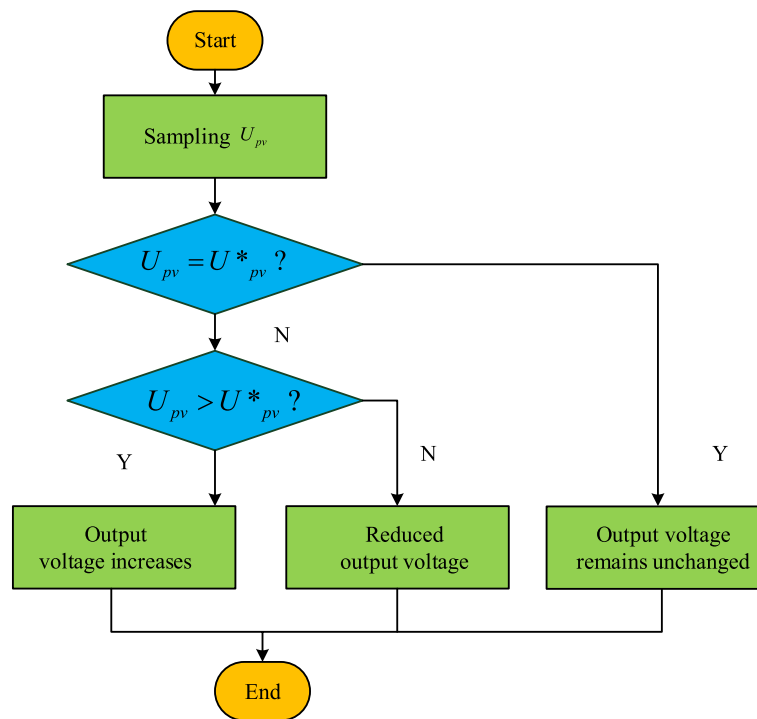
Fig. 4 Fixed voltage control diagram

in engineering. Its working principle involves adding a disturbance voltage to the PV array and recording the change in output power. Based on the results of the disturbance power change, the next direction of the disturbance is predicted and implemented multiple times to find the maximum power point. The system flow chart of the disturbance monitoring method is shown in Fig. 5.

As shown in Fig. 5, the perturbation observation method is easier to operate, has fewer variables present in the process, is uncomplicated to operate, is easy to achieve, and can be adapted to many situations. Better MMP control results can be obtained in the prevailing external environment. However, the control algorithm has the same shortcomings, so it needs to be optimized. During the process of maximum power tracking, it is important to minimize power loss for optimization. Additionally, when sunlight is enhanced, the disturbance power value may increase, causing it to be larger than the power before the disturbance. This can result in the disturbance incorrectly continuing in the same direction, leading to miscalculations and decreased system reliability. Therefore, it is necessary to reduce miscalculations. The power tracking accuracy and speed need to be improved. Both the fixed voltage method and the disturbance observation method have different advantages and disadvantages, respectively, which cannot fully satisfy the need of tracking the maximum power point, so the fixed voltage method and the disturbance observation method are combined to obtain an improved composite algorithm for maximum power tracking. The flowchart of the improved composite maximum power tracking algorithm is shown in Fig. 6.

The calculation method for the maximum power point shown in Fig. 6 is a composite control algorithm that combines the fixed voltage method and the improved step size
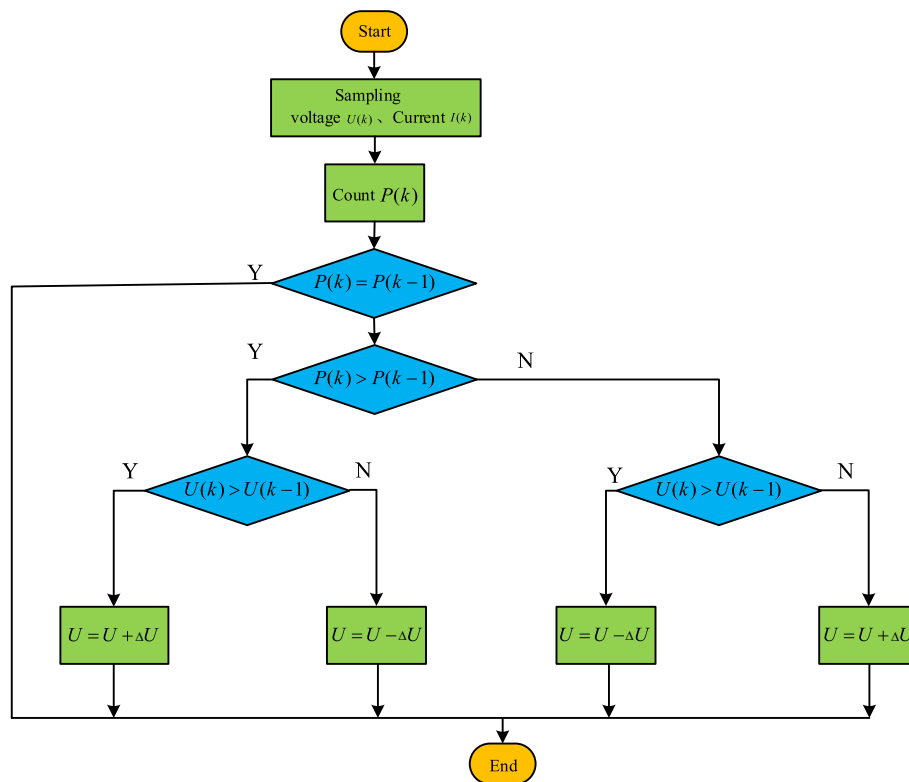
Fig. 5 Disturbance observation method control chart

disturbance method. The initial parameters are the voltage U_k and current I_k of the PV cell, and the convergence condition is that when the working point is located on the left side of the MPP point ($U_1 <$ PV output voltage $< U_2$), the disturbance step size value of the stable slope change part of the P-U output characteristic curve is set to Δd_{max}, thereby improving the tracking speed of the system; Set the disturbance step value on the left side of the MPP point where the slope of the P-U output characteristic curve changes significantly and on the right side of the maximum power point (PV output voltage $Upv > U_2$) as Δd_{min}, and the simulation platform is Simulink. At the initial stage of power tracking, the fixed voltage method (PV output voltage $U_{oc} \leq U_1$) can be used to quickly reach the vicinity of the MPP point through large steps, achieving fast tracking. Then, the variable step disturbance observation method can be used to further accurately optimize the system, ensuring real-time tracking, reducing power oscillations in the system and improving the conversion rate of solar energy. This improves the accuracy of the control system. PV grid-tie inverters can be divided into isolated type and non isolated type. The topology of both inverters is shown in Fig. 7.

Industrial Frequency Isolated Grid Inverter An AC grid inverter is a device that converts high voltage and high current industrial frequency AC power into DC power through an isolation transformer and sends DC power to the power grid after passing through a filter circuit, which is widely used in various types of power supply systems. High-frequency isolated grid-connected inverter is an isolated inverter circuit composed of three-phase fully controlled devices, which is the main device for inverting DC power
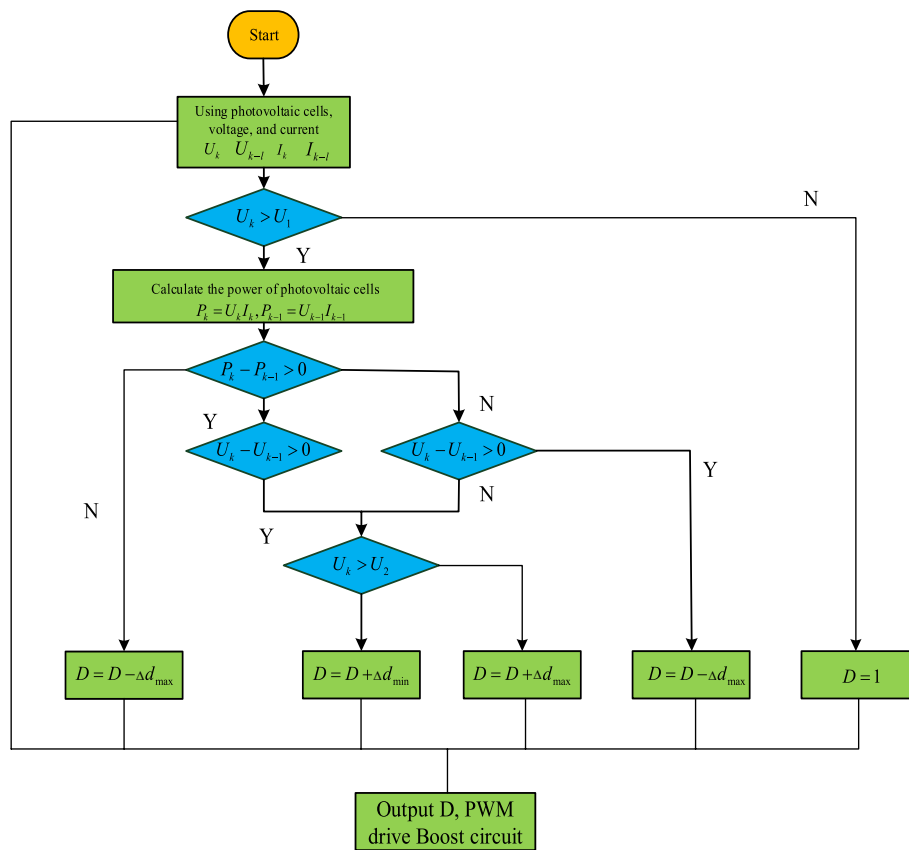
Fig. 6 Flow chart of improved composite maximum power tracking algorithm

(a)Power frequency isolated photovoltaic grid connected inverter

(b)High frequency isolated photovoltaic grid connected inverter
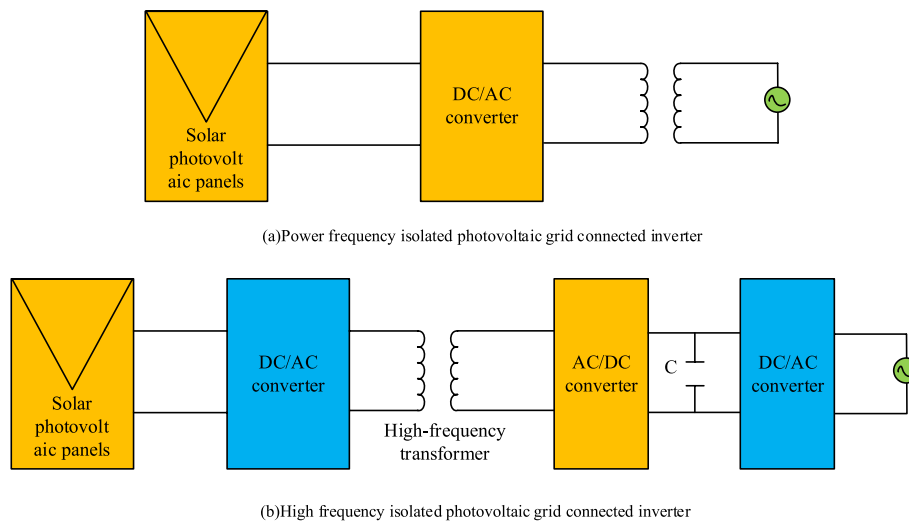
Fig. 7 Topological structure of isolated and non- isolated inverters

into AC power. High-frequency isolation is used between the isolation transformer at the output of the circuit and the input side, so the input voltage of the inverter does not affect the load. Non-isolated PV inverters can be further divided into single-stage and

multi-stage types, and multi-stage PV grid-connected inverters are mainly based on the two-stage type. Two-stage grid-connected control system, the front stage uses DC/DC converter to improve the voltage level, and at the same time can achieve MPPT control; the back stage DC/AC is converted to alternating current.

Calculation and analysis of simulation parameters for grid-connected photovoltaic systems

Experimental setup

This study utilized several pieces of experimental equipment, including a PV panel, MMC multi-level converter, grid-connected inverter, and transformer. The physical diagram of the equipment is shown in Fig. 8.

Figure 8a displays an example of the PV panel utilized in the experimental setup. The PV panel is the central component of the PV power generation system, responsible for converting solar energy into DC electrical energy. In the MMC-based optimized PV grid-connected control system, the PV panel converts solar energy into DC power and feeds it into the MMC multistage converter. Figure 8b displays an example of the MMC multistage converter utilized in the experimental setup. The MMC multistage converter is a crucial component in the system that enables voltage level enhancement and bidirectional energy flow. The topology and control strategy of the MMC multistage converter

(a) Photovoltaic panels

(b) MMC Multi-level converter

(c) Grid-connected inverter

(d) Transformer

Figure. 8 Main experimental equipment used in the institute

can be studied in the experimental setup to enhance its voltage level and energy flow in both directions. Figure 8c displays the grid-connected inverter utilized in the experimental setup. This component converts DC power to AC power, and its performance and stability have a direct impact on the grid-connected operation of the entire PV power system. Figure 8d shows an example of the transformer used in the experimental setup. The transformer plays a crucial role in the MMC-based optimized PV grid-connected control system by boosting or bucking and facilitating the interconnection between the PV power system and the grid. In the experiment, the transformer's performance and stability were modeled and simulated under various operating conditions.

The purpose of researching the optimized PV grid-connected control system based on MMC is to solve practical problems and improve the operational efficiency and stability of the PV power generation system. Therefore, when designing and constructing the experimental device, it is important to fully consider the needs and characteristics of practical applications. This will ensure that the experimental results can be effectively applied in practical scenarios, contributing to the promotion and development of the results.

Output characterization of PV array and validation of the results of the composite MPPT algorithm

When the temperature and intensity of solar radiation were under standard conditions ($S = 1000W/m^2$, $T = 20$ °C), the experimental study of solar PV cells was carried out and the voltage versus current and power versus voltage curves were obtained as shown in Fig. 9.

The PV cell in Fig. 9a is a non-constant voltage and constant current source. When the output voltage does not reach the peak value, the output current remains essentially constant. When the output voltage exceeds the peak value, the output current decreases rapidly as the voltage rises until it reaches zero. Figure 9b it can be seen that the output power increases gradually until it does not reach the maximum value, and then decreases rapidly after the maximum value is exceeded until it drops to 0. Under the condition that the intensity of solar radiation and the external ambient temperature remain constant, the output power of the system has only one extreme value. The amount of solar irradiation is a significant component that affects the PV performance of solar cells. To analyse the changes in the intensity of solar radiation, the temperature is kept at standard conditions and the power is experimented at

(a) U-I characteristic curve   (b) U-P characteristic curve
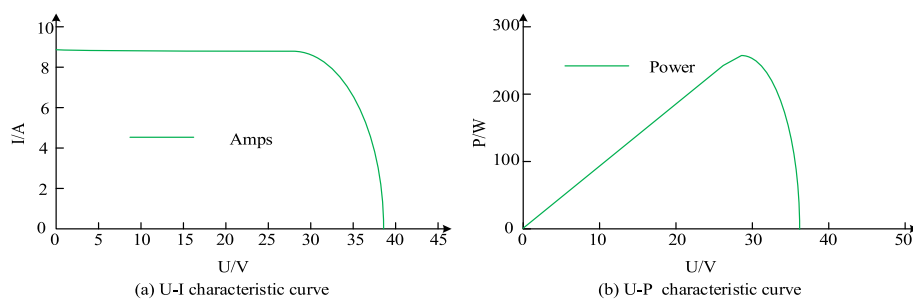
Fig. 9 U-I and P-U characteristic curves

1000, 800, 600 and 400 respectively to obtain the voltage versus current curve and the power versus voltage curve, as well as the U-I and P-U characteristics of the solar PV cell. To study the effect of temperature on the PV characteristics of the solar cell. The standard operating condition (S = 1000 W/m^2) for solar radiation intensity has been specified, and then simulation experiments have been carried out when the temperature has been set to 10 °C, 25 °C, 35 °C, 45 °C, respectively, to obtain the voltage vs. current and power vs. voltage curves of solar PV cells, i.e., U-I, P-I output characteristics.

As shown in Fig. 10, in Fig. 10a, at constant temperature, the intensity of sunlight irradiation has little effect on the open-circuit voltage of the PV cell, but the short-circuit current is affected by the large change in the intensity of sunlight irradiation. According to Fig. 10b, as the intensity of sunlight irradiation increases, the maximum power of the solar PV cell increases and changes in a wide range. So there is a nonlinear connection between the P-U and U-I output characteristic curves of the solar PV cell and the intensity of solar radiation, and the size of the solar radiation intensity can greatly affect the maximum value of the output power and the short-circuit current I_{sc}, and the open-circuit voltage U_{oc} is less affected. Figure 10c, under a certain intensity of sunlight irradiation, the open-circuit voltage of the solar cell decreases with increasing temperature, while the short-circuit current increases slightly with increasing temperature. As shown in Fig. 10d, when the intensity of sunlight irradiation S is constant, the maximum output power of the solar cell decreases slightly with increasing temperature (basically unchanged), and the value of the voltage at the time of arriving at the maximum power is also slightly reduced. The open-circuit voltage of the solar PV cell will have different degrees of changes at different temperatures, while its short-circuit current and maximum power will have different degrees of changes at different temperatures. The improved composite MPPT algorithm as well
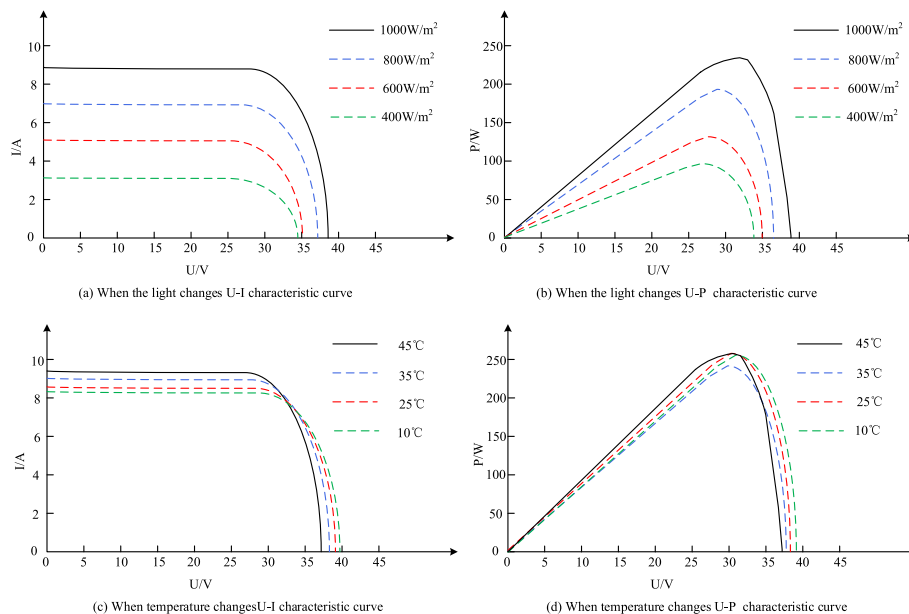
Fig. 10 U-I and P-U characteristic curves when temperature remains constant, light intensity changes, and temperature changes respectively

as the three MPPT algorithms are simulated in MATLAB software and the simulation comparison graphs obtained are shown in Fig. 11.

Using the conventional perturbation observation method, the MPP point was found to be very slow and its ripple changed significantly after stabilization. The improved composite MPPT algorithm reaches the MPP point faster than the disturbance algorithm and the constant voltage algorithm, and remains stable at the maximum power point after reaching the MPP point without any sudden changes. The constant voltage algorithm and the disturbance algorithm reach the MPP point slower than the improved algorithm, and both undergo sudden changes after reaching the maximum power point, indicating that these two algorithms are not stable after reaching the maximum power point. The improved composite MPPT algorithm can not only achieve fast maximum power tracking, but also stabilize near the maximum power point with minimal fluctuations after reaching the maximum power point. In conclusion, the improved composite MPPT algorithm has improved its performance and is feasible. Overall, the traditional disturbance observation method reaches the MPP point at 0.17 s and only reaches a stable state at 0.25 s. The fixed voltage method found the MPPS point around 0.09 s, but its stability fluctuated and reached a stable state only after 0.15 s. The improved composite control algorithm quickly found the MPP point at 0.1 s and then reached a stable state, which can not only quickly achieve maximum power tracking, but also stabilize near
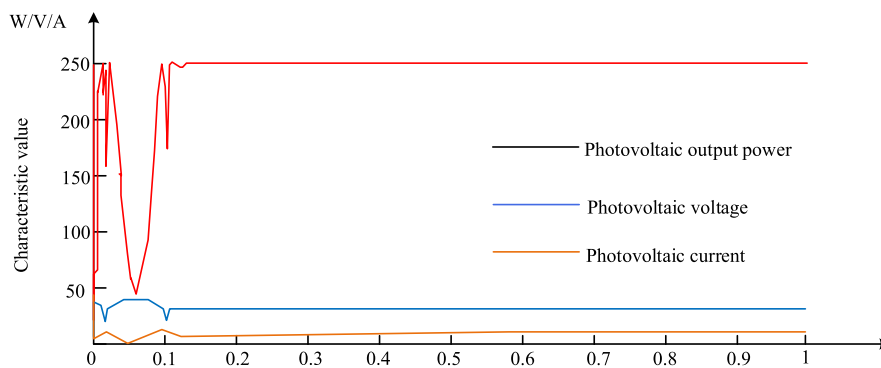
(a) Improved Composite MPPT Algorithm
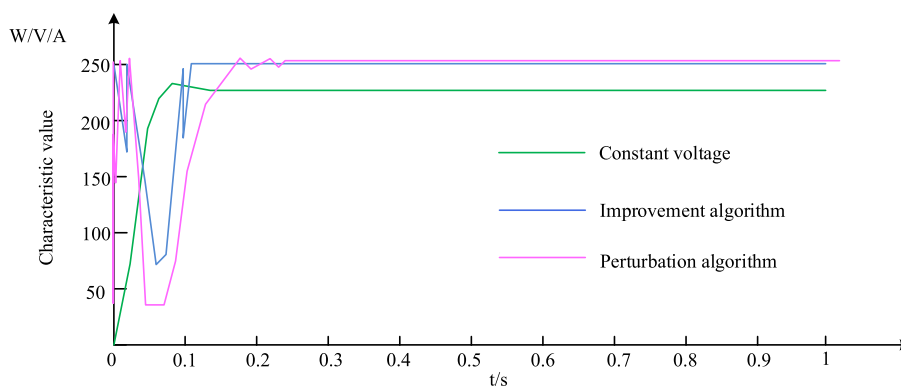
(b) Three MPPT Algorithm Tracking Maps

Fig. 11 Improved composite MPPT algorithm and simulation comparison of three MPPT algorithms

the maximum power point after reaching it with minimal fluctuations. To enhance the universality of the results, the study applied the Constant Voltage, Improvement, and Perturbation algorithms to the same dataset and recorded the tracking outcomes. This approach allows for a clearer observation of the efficiency improvement of the composite MPPT algorithm. Table 1 shows the tracking efficiency of the three algorithms.

Table 1 shows that the traditional disturbance observation method reaches the MPP point at 0.17 s, but it only achieves stability at 0.25 s. The fixed voltage method identifies the MPPS point at around 0.09 s, but its stability fluctuates and it only reaches a stable state after 0.15 s. The improved composite control algorithm quickly identifies the MPP point at 0.1 s and immediately achieves stability. Not only can it achieve maximum power tracking quickly, but it can also stabilize near the maximum power point with minimal fluctuations. Similar to the study in this paper, the conventional full-bridge DC/DC converter's IGBT has been replaced with a cascade of sub-modules in multilevel technology to enable practical applications to enhance voltage levels and allow for bi-directional energy flow. This topology can increase voltage levels and enable bidirectional energy flow.

Simulation analysis of the grid-connected system
In practical engineering, light intensity and ambient temperature are not always maintained at a fixed level, but change with climate and time. The effect of changes in light intensity on the system programme light intensity changes in the module settings, starting from 0 s, the light intensity is set to 750 W/m^2, after 0.5 s the temperature increases to 1000 W/m^2, the test temperature is set to 250 ℃. The capacitance voltage variation waveforms of the upper and lower bridge arm submodules and the voltage simulation waveforms of the DC bus are shown in 11. 10(a). The rated value of the capacitor voltage of each submodule is 1 kV and the actual value of the capacitor voltage of each submodule fluctuates up and down around 1 kV with a fluctuation range of approximately ± 40 V and a fluctuation rate of 4% as derived from the simulation. When the system starts up, the capacitor voltage of the submodule rises rapidly and then stabilizes close to the rated value. At 0.5 s, the intensity of solar radiation abruptly increases to 1000 W/m^2. As a result, the PV array enters the maximum power operating state. Additionally, the capacitive voltage of each submodule experiences a significant increase in fluctuation, with an amplitude of approximately ± 80 V and a fluctuation rate of about 8%. Despite this increase, the voltage remains close to the rated voltage. The voltage simulation waveform of the DC bus is shown in Fig. 12b, and its rated voltage level is 10 kV.

In Fig. 12b, the DC bus voltage is always kept near the rated value, and at 0.5 s, because the light radiation intensity suddenly increases from 750 to 1000 W/m^2, there is a short

Table 1 Tracking efficiency of three algorithms

Algorithm	Stabilization time/(s)	Firm power/(W)	Time to reach the maximum power point/(s)
Constant voltage	0.15	240	0.09
Improvement algorithm	0.10	250	0.10
Perturbation algorithm	0.25	250	0.17

(a)Submodule capacitor voltage

(b)DC bus side voltage
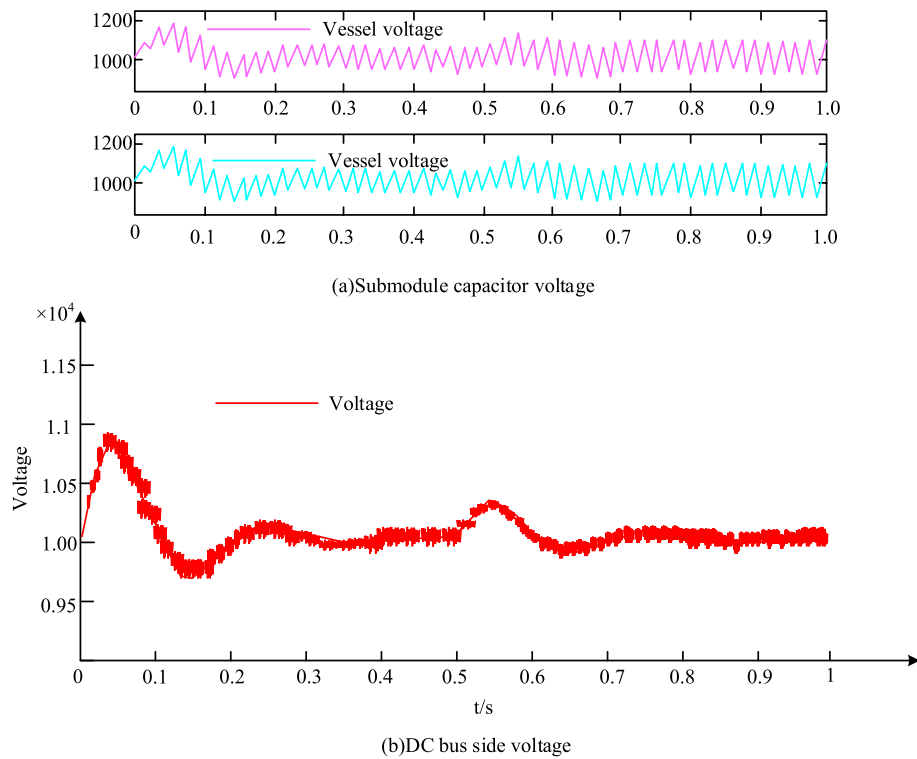
Fig. 12 Sub module capacitor voltage and DC bus side voltage

and sudden increase in the DC voltage, but then it decreases rapidly, and finally returns to stabilize near the rated voltage level. It can be ascertained that the DC bus-side voltage of this MMC PV grid-connected system can be maintained near the rated value during the continuous change of light intensity, which can ensure the stability of the whole system. The simulated waveforms of the AC inverter power output from the MMC are shown in Fig. 13.

As shown in Fig. 13, Fig. 13a shows the output active power waveform transformation diagram, in the first 0.5 s light intensity of 750 W/m^2, the output power start-up has certain fluctuations, but eventually stabilized at about 4 MW, after 0.5 s, as the light intensity increases to 1000 W/m^2, the maximum output power suddenly increases, the maximum value of the power can reach 5.4 MW, and then quickly stabilized at about 5.2 MW. Figure 13b shows the output reactive power waveform transformation diagram, the MMC outputs 0.14 MW of reactive power to compensate for the system reactive power consumption, to ensure that the total PV grid-connected power factor of 1. Simulations have verified that the PV grid-connected architecture can independently regulate the active and reactive power, and there is no need for an additional reactive power compensation device to compensate for the whole system. The output power simulation characteristic curve of a single PV array is shown in Fig. 14.

Figure 14 shows that when the light intensity is 750 W/m^2 during the first 0.5 s, the current of the individual PV array output remains steady at approximately 110 kW. When the illumination intensity is increased to 1000 W/m^2 for the next 0.5 s, the amount of electricity produced by the individual output also increases, but it remains steady. The
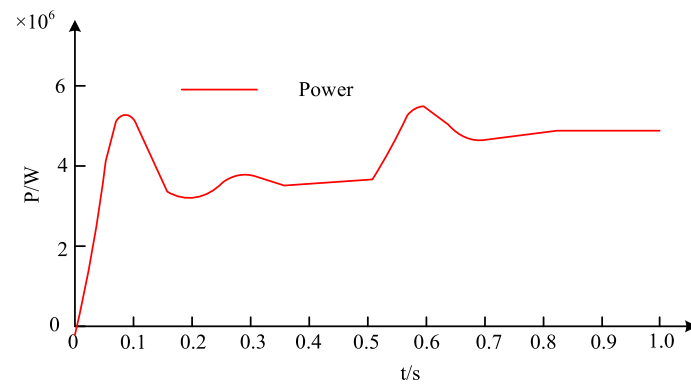
(a) Active power output by MCC
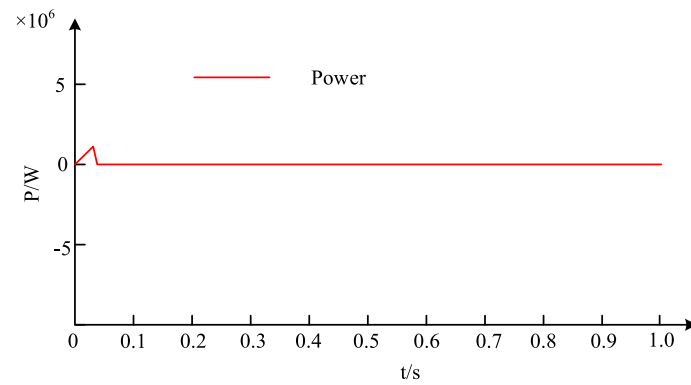
(b) Reactive power output by MCC

Fig. 13 Simulation waveform of AC inverter power output by MMC
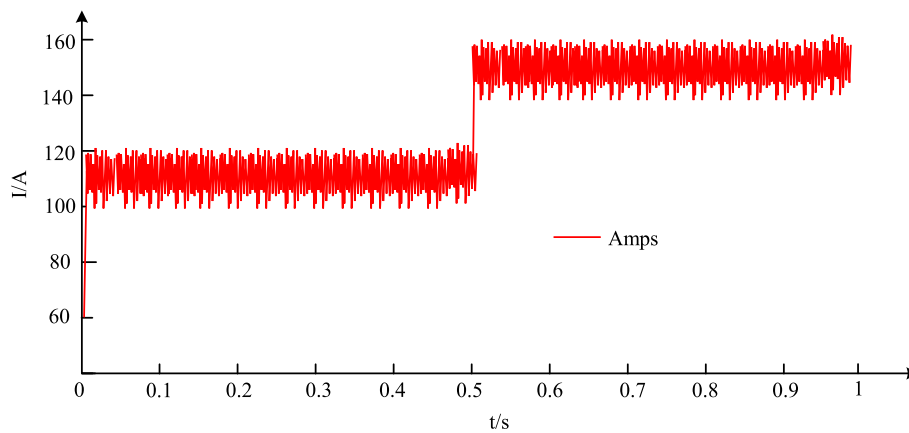
Fig. 14 Output power simulation characteristic curve of a single photovoltaic array

screenshot of the grid-connected current and reference current of PI + quasi-PR controller is shown in Fig. 15.

Figure 15a shows the FTT analysis diagram controlled by a single PI, with a current harmonic distortion rate of 3.87% for the PV grid-connected system. Figure 15b displays the FTT analysis diagram controlled by compound PI + quasi-PR, with a current

(a) Simulation wave-form graph of grid-connected current and reference current of PI controller

(b) Simulation waveform of grid connected current and reference current for PI+quasi PR controller
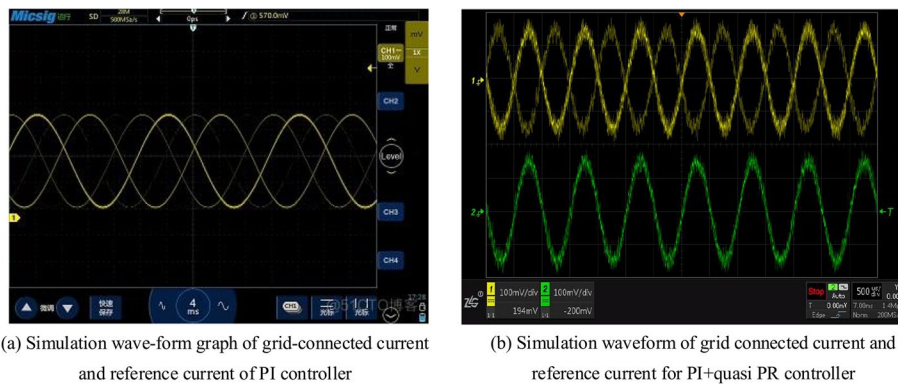
Fig. 15 Screenshot of the grid-connected current and the reference current of the PI＋quasi-PR controller

harmonic distortion rate of 1.84% for the PV grid-connected system. The harmonic content is below the 5% requirement for THD rate set by the Institute of Electrical and Electronic Engineers (IEEE). This proves that the output waveform harmonic content is very low and the pollution to the power grid is minimal when the composite control method is applied to the MMC PV grid-connected system. It is not necessary to assume that the filtering device reduces cost and footprint.

Conclusion

In the future, PV power generation has vast application prospects and development potential. It primarily utilizes solar energy to produce electricity, offering benefits of sustainability, green environmental protection, and abundant solar energy resources. However, the performance of PV power generation and its system can be impacted by various external factors. The MMC technology was implemented in the PV power generation system to enhance efficiency, optimize regulation of temperature and size of light, and improve overall performance. A composite control algorithm was proposed, which was tested experimentally and found to have better performance than traditional algorithms. The feasibility of the method was confirmed and optimization results were improved. The PV grid-connected system was tested using a combination of MMC and composite PI and quasi-PR control algorithms. It had rationality and effective control. During the simulation of output power characteristics for a single PV array, stable current output at approximately 110 kW was observed for the first 0.5 s when light intensity was set at 750 W/m^2. When the light intensity increased from 750 to 1000 W/m^2 for 0.5 s, the current output of the single array increased but remained stable. The operational efficiency of the improved composite control algorithm was represented by the time it took to reach the MPP point and remain stable, which increased from 0.25 to 0.15 s. This improvement was achieved without compromising stability. The introduction of MMC technology for PV power generation system improves the power generation efficiency, but the research results mainly come from the Simulink simulation platform, and the actual experimental data is insufficient, which can be further verified by the experimental platform in future research. The output power of PV power generation is directly affected by weather factors, such as the intensity of solar radiation and the duration of light. This may lead to stability problems of the system under different weather

conditions. Future research should aim to combine PV power generation with other renewable energy sources to improve the stability and reliability of the entire system. The novelty of this research lies in its focus on the optimized PV grid-connected control system based on MMC, which not only considers the grid-connected control of a single PV system but also its integration with other renewable energy sources.

Discussion

The optimized PV grid-connected control system based on MMC is designed with modularity, standardization, and openness in mind for its application in the Yangtze River. The modular design allows for easy expansion, and the system's processing capability can be enhanced by adding corresponding modules. Various types of PV devices, such as crystalline silicon PV cells, thin-film PV cells, and multi-junction solar cells, possess unique characteristics and performance parameters. As a result, the MMC-based optimized grid-connected PV control system must be flexible enough to accommodate different PV devices and capable of adjusting and optimizing parameters based on the specific characteristics of each device. The optimized control system for grid-connected PV using MMC technology has applications not only in PV power generation but also in the broader field of energy informatics. As the energy internet and smart grid continue to develop, the collection, transmission, processing, and utilization of energy information become increasingly important. The optimized control system for grid-connected PV using MMC is an efficient, stable, and reliable information processing and control scheme. It can provide powerful support for the acquisition, transmission, storage, and application of energy information.

Declarations

Ethics approval and consent to participate
Not applicable.

Consent for publication
Not applicable.

Competing interests
It is declared by the authors that this article is free of competing interests.

References

Chen HC, Li SS, Wu SL (2022) Hybrid energy storage module in photovoltaic power generation system for brushless DC motor operation. Sensors Mater Int J Sensor Technol 34(2 Pt.3):871–884
Gobburi HB, Borghate VB, Meshram PM (2022) Sensorless voltage balancing method for modular multilevel converter. Int J Circuit Theory Appl 50(6):65–97

Gong X, Hu S, Zhu R (2021) Multistep finite control set model predictive control of photovoltaic power generation system with harmonic compensation. Complexity 2021(21):21–30

Guo Q, Zhang X, Li J, Li J (2022) Fault diagnosis of modular multilevel converter based on adaptive chirp mode decomposition and temporal convolutional network. Eng Appl Artif Intell 107(3):45–57

Inwumoh J, Baguley C, Gunawardane K (2022) A dynamic control methodology for DC fault ride through of modular multilevel converter based high voltage direct current systems. Comput Electr Eng 100(8):40–55

Islam MM, Nagrial M, Rizk J (2021) Dual stage microgrid energy resource optimisation strategy considering renewable and battery storage systems. Int J Energy Res 45(15):21340–21364

Ju X, Liu X, Liu S, Xiao Y (2022) Optimal scheduling of wind-photovoltaic power-generation system based on a copula-based conditional value-at-risk model. Clean Energy 6(4):550–556

Lei M, Zhao C, Li Z, He J (2022) Circuit dynamics analysis and control of the full-bridge five-branch modular multilevel converter for comprehensive power quality management of Cophase railway power system. IEEE Trans Industr Electron 69(4):3278–3291

Li Y, Ye F, Liu Z, Wang Z, Mao Y (2021) A short-term photovoltaic power generation forecast method based on LSTM. Math Probl Eng 2021(3):11–21

Liu D, Liu Y, Sun K (2021) Policy impact of cancellation of wind and photovoltaic subsidy on power generation companies in China. Renew Energy 177(11):134–147

Ma X, Cheng Q, Cheng Y, Rui X, Zhao J (2021) Dual-assivity-based control strategy of modular multilevel matrix converter. Int Trans Electr Energy Syst 31(1):4–21

Naz S, Akram M, Muzammal M (2023) Group decision-making based on 2-tuple linguistic T-spherical fuzzy COPRAS method. Soft Comput 27(6):2873–2902

Noman AM, Addoweesh KE, Alabduljabbar AA (2019) Cascaded H-Bridge MLI and three-phase cascaded VSI topologies for grid-connected PV systems with distributed MPPT. Int J Photoenergy 2019(1):15–36

Pillai M (2021) Global, non-scattering solutions to the energy critical Yang-Mills problem. J Hyperbolic Differ Equ 18(1):29–141

Rugthaicharoencheep N, Maigan J (2020) Impacts of factor lightning and surge protection for photovoltaic power generator on distribution system. Appl Mech Mater 901(8):103–108

Subudhi P, Punetha D (2023) Progress, challenges, and perspectives on polymer substrates for emerging flexible solar cells: a holistic panoramic review. Prog Photovolt 31(8):753–789

Wang Y, Gao M, Wang J, Wang S, Liu J, Tan Z (2021) Measurement and key influencing factors of the economic benefits for China's photovoltaic power generation, a LCOE-based hybrid model. Renew Energy 169(5):935–952

Xiao Q, Mu Y, Jia H, Jin Y, Yu X, Teodorescu R, Guerrero J (2022a) Novel modular multilevel converter-based five-terminal MV/LV hybrid AC/DC microgrids with improved operation capability under unbalanced power distribution. Appl Energy 306(1):21–48

Xiao H, Lin C, Kou G, Peng R (2022b) Reliability modelling and configuration optimization of a photovoltaic based electric power generation system. Reliab Eng Syst Saf 220(4):51–60

Xiu G, Zhao Z (2021) Sustainable development of port economy based on intelligent system dynamics. IEEE Access 9(1):70–77

Xu K, Zhang Z, Lai Q, Yin X, Wei L (2021) Applicability study of single-phase reclosing in tie line of photovoltaic power plant. IET Gener Transm Distrib 15(6):997–1012

Ye Y, Lin M, Wang X (2020) Asymmetric cascade multilevel inverter with self-balanced switched-capacitor unit and single source. IET Power Electron 13(15):3254–3262

Publisher's Note